

RESEARCH PAPER

Carbon Black-intercalated Reduced Graphene Oxide Electrode with Graphene Oxide Separator for High-performance Supercapacitor

Hossein Jeddi¹, Reza Rasuli^{1*}, Mohammad Mahdi Ahadian², Bahareh Mehrabi²

¹Department of Physics, Faculty of Science, University of Zanjan, Zanjan, Iran

²Institute for Nanoscience and Nanotechnology (INST), Sharif University of Technology, Tehran, Iran

ARTICLE INFO

Article History:

Received 15 May 2019

Accepted 18 July 2019

Published 01 October 2019

Keywords:

Carbon Black

Reduced Graphene Oxide

Supercapacitor

ABSTRACT

We present a general study on a high performance supercapacitor based on intercalated reduced graphene oxide with carbon black nanoparticles. Graphene oxide sheets were synthesized by oxidation and exfoliation of natural graphite and were reduced using hydroiodic acid in the presence of carbon black nanoparticles. Graphene paper was fabricated by one-step procedure via simultaneous reducing and drying the aqueous solution of mixed carbon black nanoparticles and graphene oxide on a conductive substrate. Transmission electron microscopy confirmed the intercalation of carbon black nanoparticles into reduced graphene oxide sheets, preventing them from restacking during the fabrication of paper. Results confirmed that the electrochemical performance of the reduced graphene oxide paper as a supercapacitor electrode was improved by intercalation of carbon black nanoparticles into reduced graphene oxide sheets and also the assembled supercapacitor becomes more efficient with graphene oxide separator. Cyclic voltammetry of the prepared electrodes in 30 wt% KOH solution at 10 mV/s scan rate showed that adding only 5 wt% of carbon black to graphene oxide increases specific capacitance from ~118 F/g to 129 F/g. In addition, the maximum specific capacitance (139 F/g) was obtained by adding 15 wt% of carbon black and that increased to 142 F/g by the use of graphene oxide paper as a separator. Furthermore, electrochemical impedance spectroscopy by Nyquist plot showed that charge transfer resistance in electrodes decreases from 18 Ω in the reduced graphene oxide to 6 Ω in the reduced graphene oxide paper with intercalated carbon black nanoparticles and ions diffusion occurs easier than previous.

How to cite this article

Jeddi H, Rasuli R, Ahadian MM, Mehrabi B. Carbon Black-intercalated Reduced Graphene Oxide Electrode with Graphene Oxide Separator for High-performance Supercapacitor. J Nanostruct, 2019; 9(4): 639-649. DOI: 10.22052/JNS.2019.04.006

INTRODUCTION

Since the first isolation of graphene in 2004, graphene-based supercapacitors have attracted remarkable attention due to the capability of energy storage and delivery [1-5]. A supercapacitor is a conventional capacitor with higher capacitance for energy storage by values more than hundreds of times per unit mass. Advantages of these devices such as long cyclic life, short charge/discharge time, high capacitance and power motivate researchers to explore their capacitance and stability [4-7].

Supercapacitors store energy by electrical double layer capacitance or pseudocapacitance and these devices are often fabricated based on carbon materials, including activated carbon, carbon nanotube and graphene due to their special properties such as high surface area, relatively low cost, non-toxicity, high chemical stability and wide temperature range [8-11].

Graphene with high surface to volume ratio (theoretical 2630 m²/g), high charge carrier mobility as well as its chemical stability has been

* Corresponding Author Email: r_rasuli@znu.ac.ir

subject of recent research for application in flexible electrodes [3, 12]. Composites of metal oxides and graphene or carbon nanotube are interesting materials for electrodes of pseudocapacitors and hybrid capacitors which contribute in redox reactions and increase specific capacitance [13-16]. Over the last few years, it has been reported that mixture of graphene and conductive polymers can enhance capacitance and energy density of electrodes considerably. For example, doping polyaniline with graphene quantum dot exhibit a specific capacitance value of ~ 1044 F/g by a current density of 1 A/g as well as better stability [17]. Also, fabrication of electrodes using functionalized microporous carbon shows high specific capacitance and good stability [18]. Recently, binder-free graphene-based papers have been applied in electrodes of supercapacitors due to their low weight and flexibility [3-5]. Facile and cost-effective method for fabrication of a high-performance electrode is a challenge in the field of supercapacitors. Several methods have been proposed for fabrication of graphene-based supercapacitor electrodes [19]. Exfoliation and then restacking of two-dimensional layered materials has attracted remarkable attention for fabrication of high performance electrodes [20, 21]. A common method is vacuum filtration deposition of graphene suspension to fabricate graphene-based electrode for supercapacitor [22]. Intercalation of ions into layered materials is another approach for fabrication of nanodevices for energy storage, including capacitors and batteries [20, 21, 23]. The interconnecting of carbon nanotubes and graphene is a novel approach to fabricate high-performance materials [24]. It has been reported that improvement in capacitance of supercapacitors based on reduced graphene oxide (RGO) is due to the adsorption of cations to the surface of sheets, while intercalation of carbon nanotubes improves the capacitance and cyclic stability in comparison with electrode based on the pure RGO [24]. However, fabrication of a stable, high-performance electrode with low resistance by a one-step and low cost method is a challenge yet.

In order to use graphene as a primal material for fabrication of the electrode, it is important to be produced by a facile and cost-effective method. A typical and low-cost approach for mass production of graphene is chemical method which includes oxidation and exfoliations of natural graphite. This method produces graphene oxide which is

a graphene with oxygen functional groups on its edges and basal planes [25]. Another challenge in the fabrication of graphene based electrodes is the reduction process. Although several reducing agents such as hydrogen sulfide, hydrazine, NaBH_4 , dimethylhydrazine, hydroquinone were reported to reduce the graphene oxide, non-toxicity, efficiency and cost of the reducing agent should be considered. It has been reported that hydroiodic acid is an efficient reducing agent to obtain RGO paper with high conductivity [26]. Hydroiodic acid reduces graphene oxide paper by replacing the oxygen functional groups with organohalides and produces high-quality RGO paper [26]. A hindrance for application of graphene as an electrode of supercapacitor is restacking of the sheets. Reducing graphene oxide during electrode preparation prevents RGO sheets from crumpling and restacking, which improves the performance of supercapacitor. In addition, separator of a supercapacitor should be electrically dielectric, but ion permeable. It seems that using graphene oxide (GO) with 10^{12} Ω/sq resistance as a separator can make supercapacitor fabrication more cost-effective and facile with high performance [23]. Another determining factor in performance, energy density and capacitance of supercapacitors is electrolyte. It has been suggested that higher capacitance could be achieved in aqueous alkaline or acid solutions compared with organic electrolytes [27]. Alkaline electrolytes such as NaOH and KOH have several advantages such as high ionic conductivity, high thermal stability, low cost, inflammability and non-toxicity that make them suitable candidates as electrolytes for supercapacitors.

In this research, we present a facile and one-step method to fabricate high performance RGO-based electrode for supercapacitor. Prepared graphene oxide sheets were reduced by chemical method using hydroiodic acid. The electrodes were fabricated by drying the carbon black (CB) nanoparticles-graphene solution. We investigated the effect of intercalation of CB nanoparticles between RGO sheets in electrochemical performance using electrochemical impedance spectroscopy (EIS) and cyclic voltammetry (CV). In addition, the application of graphene oxide paper as a separator was examined.

MATERIALS AND METHODS

GO synthesis

GO was synthesized using Hummers' and Offman method [28-30]. This method was

performed by adding 46 mL H_2SO_4 to 1 g of natural graphite (Asbury Carbons, USA) and then was stirred at 80°C for 1 h. Then 1 g NaNO_3 was added to the solution under stirring condition in an ice bath. As the solution was stirring, 4g KMnO_4 was added slowly. The solution was reached to room temperature, then was placed in an oil bath at 40°C and was stirred for 1.5 h. The solution was heated up to 90°C and then diluted by 280 mL deionized water. Finally, 6 mL H_2O_2 was added to reduce residual KMnO_4 . The residual acids and salts were removed by washing and filtering. The exfoliated sheets were separated by centrifugation at 4000 RPM for 20 min.

Electrode and GO paper fabrication

In order to reduce graphene oxide, 0.5 mL HI (57% Merck) was added to 5 mL GO (6 mg/mL) and was stirred for 30 min. Then the solution was coated on a steel sheet (0.1 mm in thickness and 2.6 cm in diameter) as current a collector and was dried at 90°C for 2 h. After drying, the electrodes were washed with acetone and deionized water. In the case of pillared RGO, 5 wt%, 15 wt% and 20 wt% of CB nanoparticles (Degussa D-60287, Germany) were dispersed in dimethylformamide by the aid of 30 min sonication and were added to the GO solution under the stirring condition before adding HI. When the electrodes were fabricated by casting method with 5 mg mass loading, supercapacitors were assembled by prepared electrodes using two kinds of separators of filter paper (filtraTech) and GO paper with the thickness of 50 μm . The GO paper was prepared by vacuum filtration of 4 mL of GO (5mg/mL) through filter film (0.45 μm pore size and 45mm in diameter). Following this, the GO paper on the filter was dried in oven for 2h at 60°C and then peeled from the filter.

Characterization

Electrochemical capacitance performance of supercapacitor electrodes was investigated by cyclic voltammetry (CV), galvanostatic charge/discharge (GCD) and electrochemical impedance spectroscopy (EIS) by the use of a potentiostat from PGSTAT Autolab in 30 wt% KOH electrolyte. EIS measurements were performed using a 0.1 V DC bias voltage with a sinusoidal signal with the amplitude of 5 mV in the frequency ranged from 1 mHz to 10 kHz. Raman spectroscopy was carried out at room temperature using Almega Thermo Nicolet Dispersive Raman Spectrometer

with excitation wavelength of 532 nm. Fourier transform infrared (FTIR) analyses were performed using Bruker-tensor27. The microstructure and morphology of the RGO and RGO/CB electrodes before and after the electrochemical tests were characterized by scanning electron microscopy (SEM) using Tescan Mira II and transmission electron microscopy (TEM) using Zeiss - EM10C at voltage of 80 kV. In addition, structure of RGO/CB was studied by x-ray diffraction (XRD) using PHILIPS-binary diffractometer by a Cu anode in the range of 5° - 80° . Size of CB nanoparticles was measured by dynamic light scattering (DLS) method using Malvern instrument. The N_2 adsorption-desorption isotherms of the samples were measured at 77 K using Belsorp mini II (BEL, Japan) to determine the specific surface areas. The specific surface area was calculated from the Brunauer-Emmett-Teller (BET) plot of the nitrogen adsorption isotherm.

RESULTS AND DISCUSSION

Raman spectroscopy was utilized to explore the layer number and the crystal quality of GO sheets. There are two significant peaks in Raman spectra of the carbon materials so-called G and D band which appear at $\sim 1580\text{ cm}^{-1}$ and $\sim 1350\text{ cm}^{-1}$, respectively [29]. The G band usually is attributed to the E_{2g} phonon of graphitized structure and the D band is corresponds to breathing mode of κ -point phonons of A_{1g} which is related to the disorder and defects [31-33]. In Raman spectra, peak position is dependent on graphene layers. G band of single layer graphene (1585 cm^{-1}) shifts about 6 cm^{-1} to lower frequencies after stacking more graphene layers. Also, 2D band of single layer graphene located at 2679 cm^{-1} is sensitive to the number of graphene layers and shifts about 19 cm^{-1} into the larger wavenumbers [29, 31-33]. It is well known that the 2D/G intensity ratio of single, double, triple and multi (>4) layer graphene is typically greater than 1.6, 0.8, 0.3 and 0.07 respectively [32, 33]. Fig. 1 shows Raman spectra of synthesized graphene oxide and RGO with 15 %wt intercalated CB. The I_{2D}/I_G ratio of 0.19 shows that mean layer number of GO is about 4. According to the figure, the G and the D peaks appear at $\sim 1630\text{ cm}^{-1}$ and $\sim 1380\text{ cm}^{-1}$, respectively. The I_D/I_G ratio increases from ~ 0.97 to ~ 1.56 and I_{2D}/I_G ratio decreases from 0.19 to 0.16 by intercalation of CB nanoparticles, which illustrates an increase in sp^3 hybridization due to the presence of CB nanoparticles and defect creation.

FTIR spectroscopy has been utilized to examine the reduction of GO by hydroiodic acid and the chemical components of the electrode materials before and after electrochemical tests. In a typical spectrum of GO, the stretching mode of hydroxyl, carbonyl (C=O) and epoxide (C–O) appears at ~ 3450 , ~ 1728 and ~ 1061 cm^{-1} respectively [29, 34]. Fig. 2 demonstrates the FTIR spectra of GO and RGO. It is obvious that all the peaks related to functional groups have been eliminated in RGO spectra and this verifies the reduction of GO. FTIR spectra of RGO and RGO/CB electrodes before and after the electrochemical tests were presented in Fig. 3. No significant changes are seen in the number of peaks in the FTIR spectra of RGO electrode after

the electrochemical tests. However, it is clear that three peaks are appeared in the spectra of RGO/CB electrode after the electrochemical tests in 661 cm^{-1} , which are attributed to O_1CO_2 bending modes, 702 cm^{-1} related to C=O in-plane bending modes coupled with O...H stretching modes and the peak at 831 cm^{-1} is due to out-of-plane bending mode of the CO_3 skeleton which are undoubtedly because of the effect of KOH on RGO/CB [35]. According to the FTIR spectra of RGO/CB electrode after the test, it could be concluded that a KHCO_3 structure is formed from the mixture of KOH and RGO/CB [35]. This phenomenon could be explained by the presence of carbon black nanoparticles in RGO/CB electrode which not only play an important

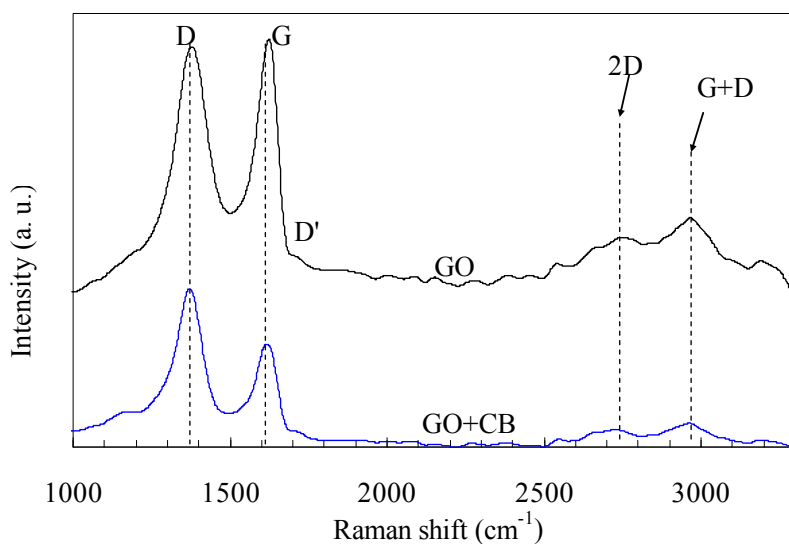


Fig. 1. Raman spectra of as-prepared GO and intercalated GO with 15%wt CB.

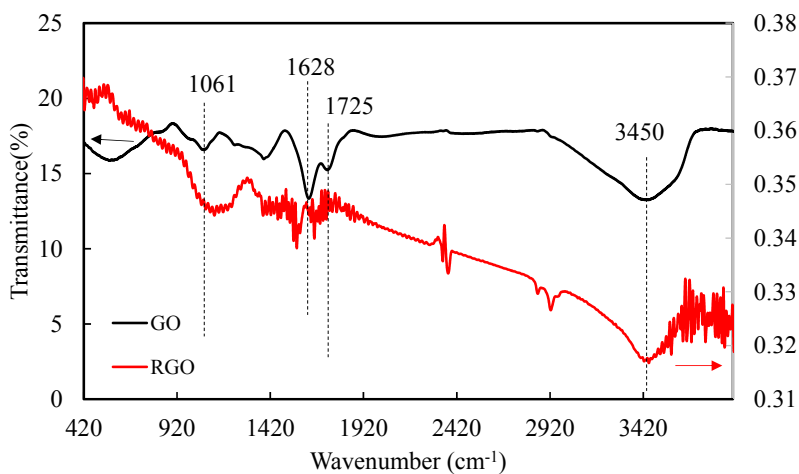


Fig. 2. FTIR spectra of as-prepared GO and RGO. The RGO has been reduced by hydroiodic acid.

role in the absorption of KOH, but also could be an effective factor in the formation of new functional groups. XRD analyses of RGO/CB electrodes before and after the electrochemical tests are shown in Fig. 4. In the XRD pattern of the RGO/CB electrode before the tests there is a small peak at 12° which could be attributed to GO and might be because of functional group as a result of incomplete reduction. Also there is a sharp peak at 24° due to RGO/CB [36]. However, XRD pattern for the RGO/CB electrode after tests confirms the structure of KHCO_3 . Table 1 and 2 present XRD data for the RGO/

Table 1. XRD data for the RGO/CB electrode after the electrochemical tests.

2θ	I / I ₀	2θ	I/I ₀
24.4	46.48	40.83	36.45
30.26	91.39	44.72	37.81
31.47	100	46.35	5.77
32.06	22.67	49.68	18.14
34.35	37.54	50.91	12.18
37.98	21.03	60.94	13.48
39.41	41.86	67.99	3.83

CB electrode after test and XRD data for KHCO_3 crystal, respectively [35]. The microstructure

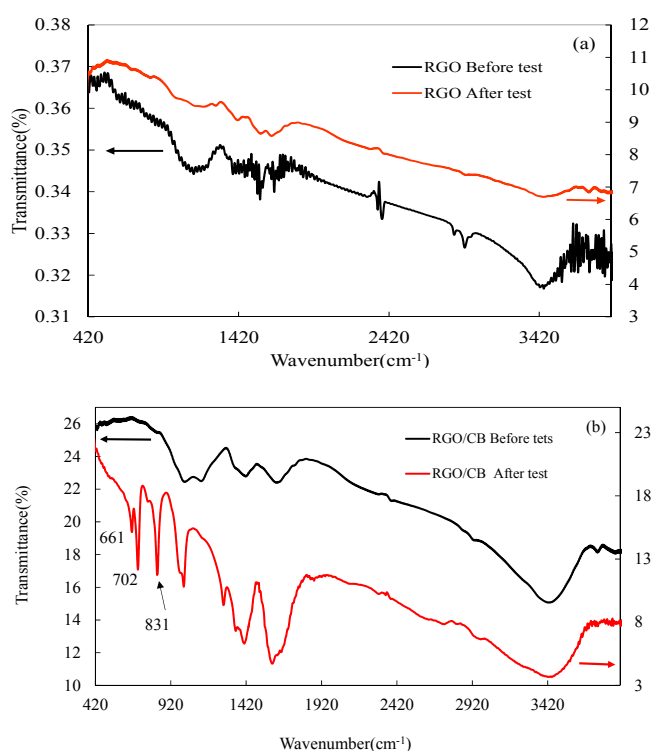


Fig. 3. FTIR spectra of as-prepared (a) RGO and (b) RGO/CB electrodes.

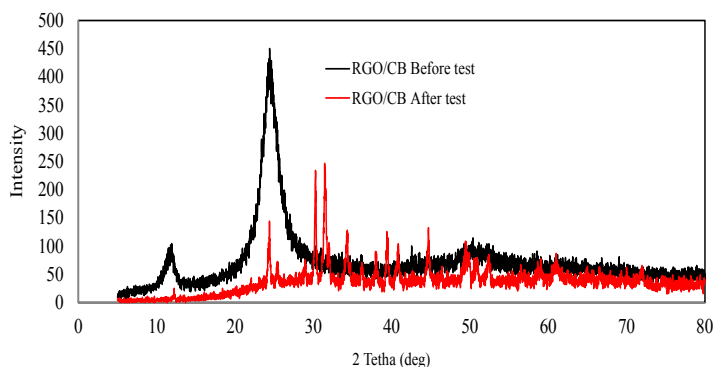


Fig. 4. XRD pattern of RGO/CB electrode

and morphology of RGO and RGO/CB electrodes before and after the electrochemical tests were characterized by SEM and TEM. According to SEM images in Fig. 5, it is clear that morphology of the electrodes becomes more porous by adding CB nanoparticles. This porous structure facilitates electrolyte ions absorption, causing to higher capacitance. Furthermore, it can be seen from the SEM images that the microstructure and morphology of the electrodes do not modify during the electrochemical tests. As shown in

TEM image (Fig. 6(a)) there is a flat RGO sheet with some wrinkles on its surface, however in Fig. 6(b) nanoparticles were distributed on the RGO sheets, preventing them from restacking. By restacking RGO sheets in the electrode, effective surface is reduced and ions cannot move between the sheets. Consequently, restacking of RGO sheets affects performance of supercapacitor by an increase in charge/discharge time and a decrease in capacity. The prepared RGO paper and supercapacitor are presented in Fig. 6(c) and 6(d).

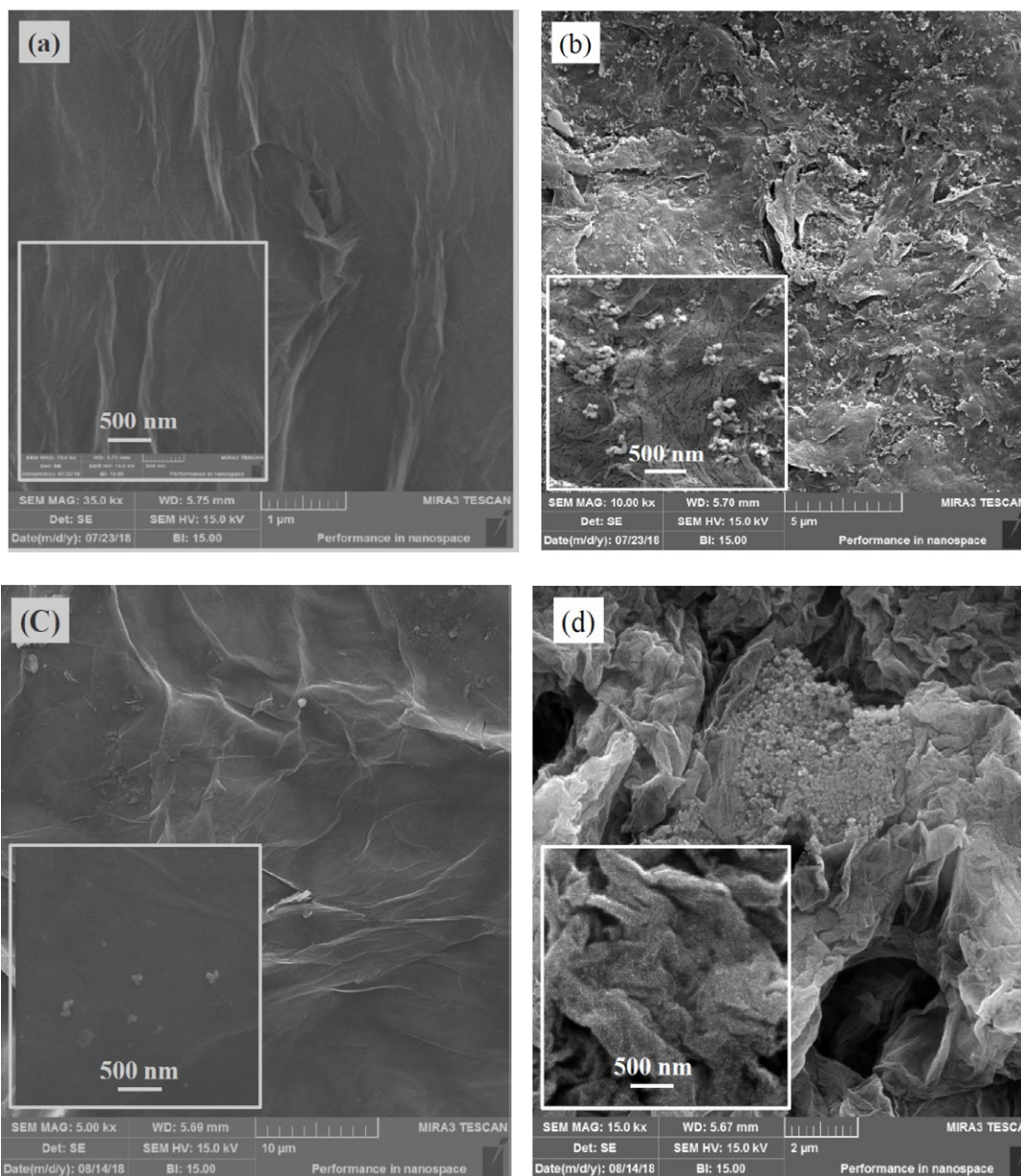


Fig. 5. SEM image of (a) RGO and (b) RGO/CB electrode before the electrochemical tests, (c) RGO and (d) RGO/CB electrode after the electrochemical tests.

In order to measure the size of carbon black nanoparticles, DLS analysis was performed. Based on Fig. 6(c), the mean particle size of the CB is about 90 nm which is more than the TEM results. Hydrodynamic radius of nanoparticles in DLS measurements is typically greater than the real size of nanoparticles and therefore we expect the greater size for CB nanoparticles by DLS. Nevertheless, as shown in the TEM image most of the CB nanoparticles have a size of about 12 nm. However, the increase in the DLS particle size cannot only be due to the hydrodynamic radius.

Therefore comparing particle size for TEM and DLS results indicates that few nanoparticles can agglomerate on graphene sheets.

CV is a powerful method to examine the performance and capacity of the prepared supercapacitor. As shown in Fig. 7, CV diagrams were broadened by increasing the scan rate. At higher scan rates more ions move toward the electrodes, resulting in higher current and wider CV diagram. As presented in Fig. 7, there is no Faradic peak in CV diagrams and charge storage occurs electro-statically. However, the CV diagram in Fig.

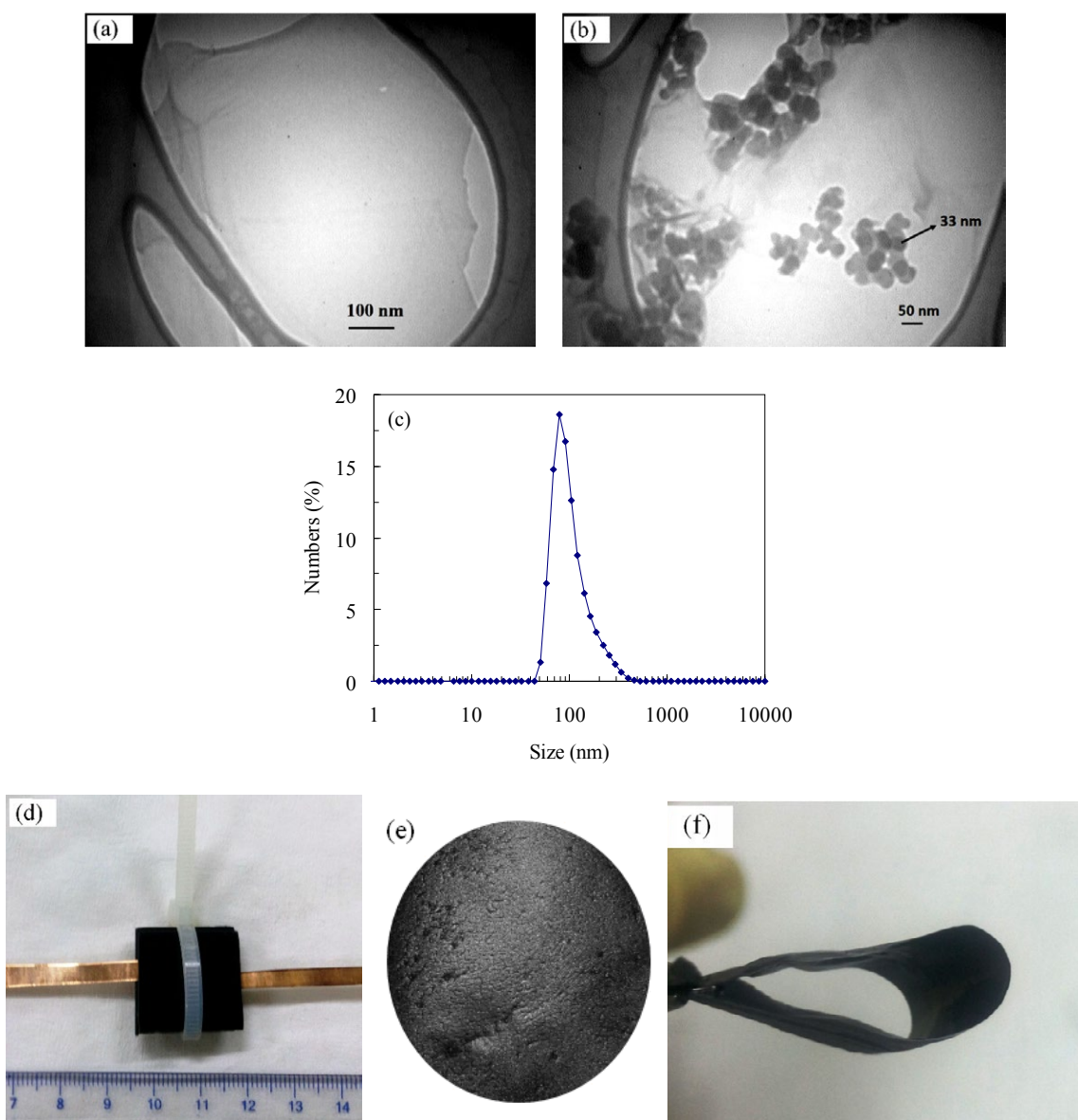


Fig. 6. TEM image of (a) RGO, (b) intercalated RGO, (c) DLS analysis of CB, (d) assembled two electrodes system supercapacitor and (e) as prepared GOP, (f) the highly flexible and mechanically robust as-prepared RGO paper.

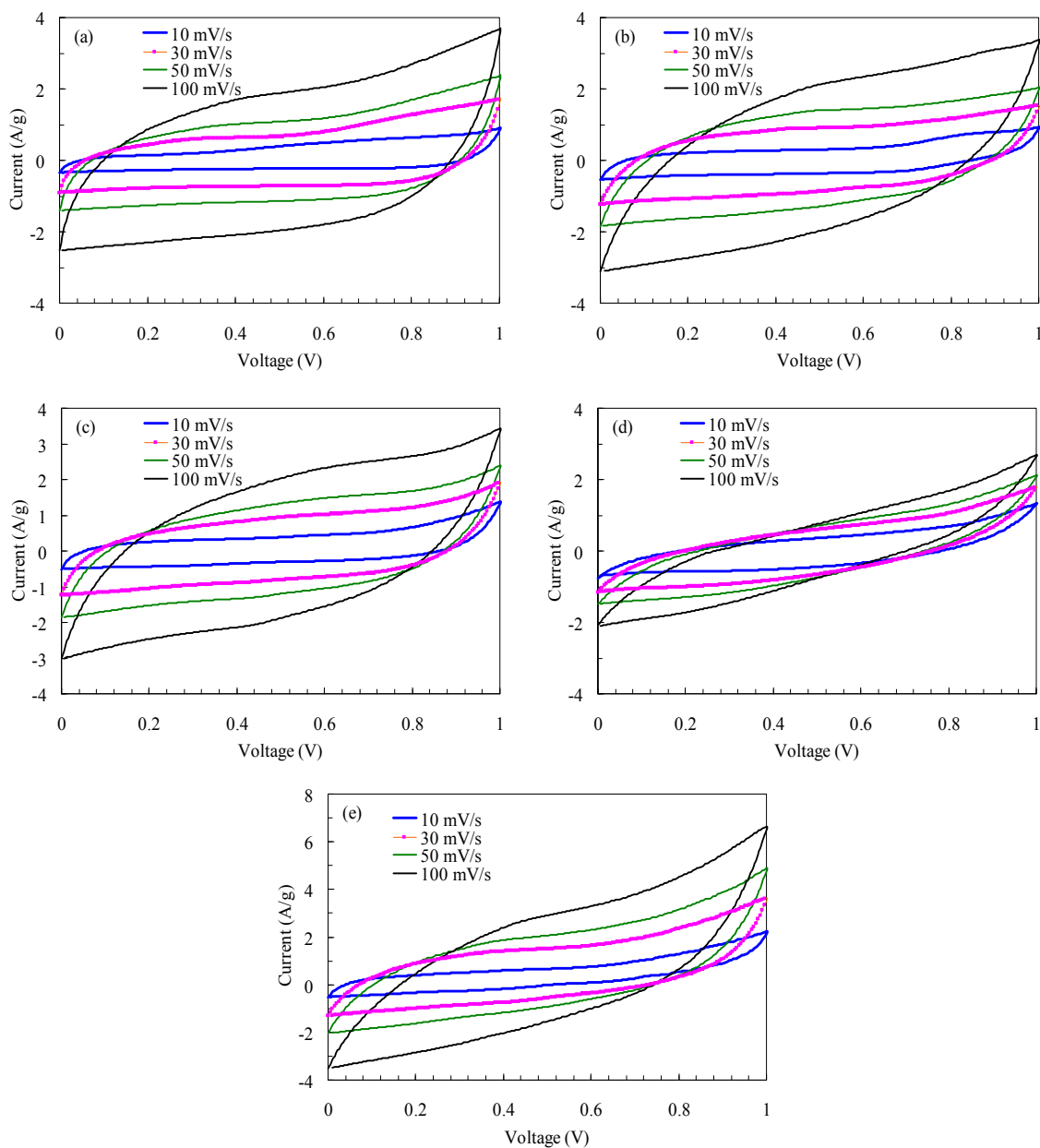


Fig. 7. Electrochemical performances of supercapacitor cells based on the RGO papers using a using 30% KOH aqueous solution as electrolyte at room temperature. CV diagrams at different scan rates for (a) RGO electrode, (b) G+5%CB, (c) G+15%CB, (d) G+20%CB, (e) GOP separator

7(d) was not broadened by increasing the scan rate which indicates the weak capacitive behavior of sample G+20% CB. To discuss quantitatively, the specific capacitances were calculated by use of CV curve via the following formula [37]:

$$C_{sp} = \frac{2 \int I(V) dV}{m \nu (V_2 - V_1)} \quad (1)$$

where V_1 and V_2 are the first and the second

Table 2. XRD data for KHCO_3 [35].

2θ	I/I_0	h k l	2θ	I/I_0	h k l
24.2	78	4 0 0	40.6	36	0 2 1
30.07	100	4 0 1	44.4	27	2 2 1
31.2	91	3 1 1	46	10	7 1 0
31.3	96	1 1 1	49.3	29	6 2 0
34.09	53	4 1 1	50.8	10	0 0 2
38.8	35	5 1 1	60.6	8	5 3 1
38.9	1	6 0 1	69.3	3	9 1 2

potential ($V_1=0$ and $V_2=1V$) and I , m and ν are current, mass of each electrode (~5 mg) and scan rate, respectively. The calculated specific capacitances are presented in Fig. 8(a). As shown in this figure, at the scan rate of 10 mV/s the specific capacitance was calculated to be 118, 129, 139 and 125 F/g for intercalated RGO with 0, 5, 15, 20 wt% CB, respectively. Furthermore, the specific surface area measured by BET. Results show that RGO/CB is increased by 823%. This indicates that CB particles as nanoscale spacers can significantly decrease the agglomeration of graphene with high

electrochemical utilization of graphene layers.

We also obtained 142 F/g by use of GO paper as a separator. Results revealed that the concentration of CB and GO paper separator are important factors for specific capacitance. The highest value of specific capacitance obtained for 15 wt% CB intercalated into RGO sheets. It means that CB nanoparticles act as spacers between the RGO sheets and also increase the conduction of electrodes with no rule in the formation of double layer, while adding more amount of CB decreases the specific capacity. In addition, the charge-

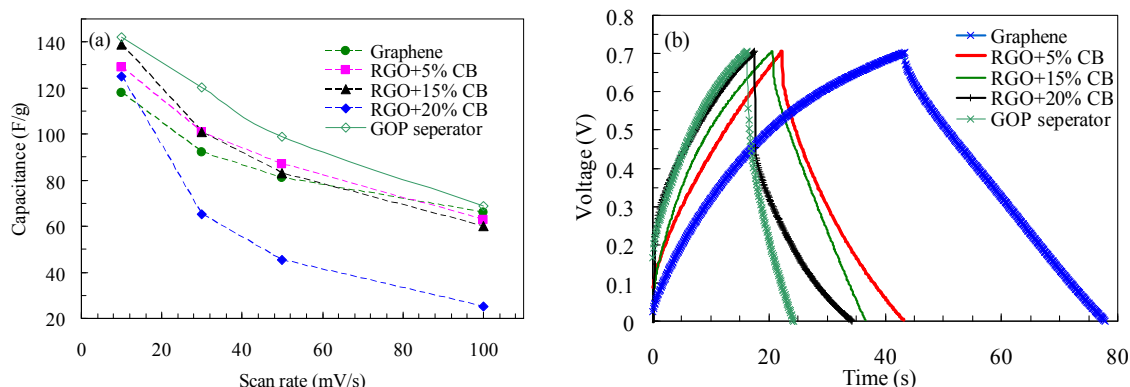


Fig. 8. (a) Specific capacitance at different scan rate and (b) Galvanostatic charge/discharge curves measured at the current density of 1A/g for RGO electrode, G+5%CB, G+15%CB, G+20% CB and GOP separator

Table 3. Comparison of RGO/CB 15 wt% with other reported researches

Active material	Electrolyte	Capacitance	Ref
Graphene/Carbon black	6 M KOH	175 F/g at 10 mV/s	[36]
Graphene/Carbon Nanotube	1M KCl	190 F/g at 0.5 A/g	[27]
Graphene/Carbon black	1 M of H ₂ SO ₄	112 F/g at 5 mV/s	[37]
Graphene/Carbon black	6 M KOH	138 F/g at 10 mV/s	[39]
Graphene/Carbon black	30 wt% KOH	139 F/g at 10 mV/s	This work

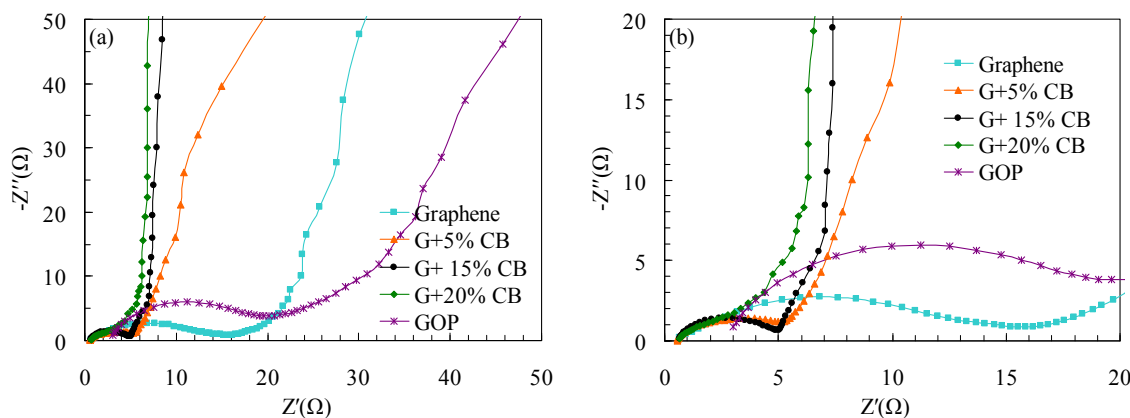


Fig. 9. Nyquist plots collected by EIS of RGO electrode, G+5%CB, G+15%CB, G+20% CB and GOP separator (b) Zoomed area of (a).

discharge diagrams of the prepared samples were measured to explore the time of charging and discharging. Fig. 8(b) indicates that the time of charging for RGO-based supercapacitor is about twice that of the RGO/CB and the supercapacitor with GO paper separator has the lowest charge time. This can be due to a decrease in the electrode resistance by CB intercalation which also increases the porosity of electrodes. The intercalation of CB nanoparticles into RGO sheets makes a porous structure which facilitates the electrolyte ion movement, but also increases conductivity of the electrodes significantly, leading to decrease in measured resistance.

Resistivity behaviors of fabricated electrodes were examined by EIS measurements. Fig. 9 demonstrates Nyquist plots, i.e. the relationship between real (Z') and imaginary ($-Z''$) part of impedance for supercapacitor. In the Nyquist plot, there is a semicircle at high frequencies and an approximately a straight line at low frequencies. The first point of the semicircle is the resistance of electrolyte and the diameter of the semicircle is charge transfer resistance. The straight line is related to Warburg resistance steamed from diffusion of ions [37, 38]. As explained, intercalation of CB nanoparticles into RGO sheets causes more conductivity between the electrodes. The semicircle parts of the Nyquist plot for electrodes with different percent of CB are compared in Fig. 9(b). Results show that by increasing the amount of CB, diameter of semicircle becomes smaller, meaning more conductivity in the electrodes.

CONCLUSIONS

We presented a facile method to improve performance of RGO based supercapacitor. Prepared RGO sheets were reduced chemically using hydroiodic acid. RGO paper was fabricated by drying and reducing the CB nanoparticles-RGO solution. We showed that the intercalation of CB nanoparticles into RGO sheets and use of GO as separator improves electrochemical performance of RGO paper and highest capacitance is obtained for RGO+15%wt CB. The electrochemical behavior of prepared electrodes was tested in 30wt% KOH solution and results verified that specific capacitance can increase from 118 to ~139 F/g and charge-discharge time becomes roughly half. In addition, EIS showed that electrode resistance decreases from 18Ω to $\sim 6\Omega$ and also ions diffusion occurs easily in the prepared electrodes.

CONFLICT OF INTEREST

The authors declare that there are no conflicts of interest regarding the publication of this manuscript.

REFERENCES

1. Wang Y, Shi Z, Huang Y, Ma Y, Wang C, Chen M, et al. Supercapacitor Devices Based on Graphene Materials. *The Journal of Physical Chemistry C*. 2009;113(30):13103-7.
2. Zhu Y, Murali S, Stoller MD, Ganesh KJ, Cai W, Ferreira PJ, et al. Carbon-Based Supercapacitors Produced by Activation of Graphene. *Science*. 2011;332(6037):1537-41.
3. Shao Y, El-Kady MF, Wang LJ, Zhang Q, Li Y, Wang H, et al. Graphene-based materials for flexible supercapacitors. *Chemical Society Reviews*. 2015;44(11):3639-65.
4. Raccichini R, Varzi A, Passerini S, Scrosati B. The role of graphene for electrochemical energy storage. *Nature Materials*. 2014;14(3):271-9.
5. El-Kady MF, Shao Y, Kaner RB. Graphene for batteries, supercapacitors and beyond. *Nature Reviews Materials*. 2016;1(7).
6. Park D-W, Cañas NA, Schwan M, Milow B, Ratke L, Friedrich KA. A dual mesopore C-aerogel electrode for a high energy density supercapacitor. *Current Applied Physics*. 2016;16(6):658-64.
7. Han S-J, Kim Y-H, Kim K-S, Park S-J. A study on high electrochemical capacitance of ion exchange resin-based activated carbons for supercapacitor. *Current Applied Physics*. 2012;12(4):1039-44.
8. Fisher RA, Watt MR, Konjeti R, Ready WJ. Atomic Layer Deposition of Titanium Oxide for Pseudocapacitive Functionalization of Vertically-Aligned Carbon Nanotube Supercapacitor Electrodes. *ECS Journal of Solid State Science and Technology*. 2014;4(2):M1-M5.
9. Redondo E, Carretero-González J, Goikolea E, Ségolini J, Mysyk R. Effect of pore texture on performance of activated carbon supercapacitor electrodes derived from olive pits. *Electrochimica Acta*. 2015;160:178-84.
10. Xu S, Wei G, Li J, Ji Y, Klyui N, Izotov V, et al. Binder-free Ti₃C₂T_x MXene electrode film for supercapacitor produced by electrophoretic deposition method. *Chemical Engineering Journal*. 2017;317:1026-36.
11. Thirumal V, Pandurangan A, Jayavel R, Krishnamoorthi SR, Ilangovan R. Synthesis of nitrogen doped coiled double walled carbon nanotubes by chemical vapor deposition method for supercapacitor applications. *Current Applied Physics*. 2016;16(8):816-25.
12. Luo J, Zhang W, Yuan H, Jin C, Zhang L, Huang H, et al. Pillared Structure Design of MXene with Ultralarge Interlayer Spacing for High-Performance Lithium-Ion Capacitors. *ACS Nano*. 2017;11(3):2459-69.
13. Masjedi-Arani M, Salavati-Niasari M. Novel synthesis of Zn₂GeO₄/graphene nanocomposite for enhanced electrochemical hydrogen storage performance. *International Journal of Hydrogen Energy*. 2017;42(27):17184-91.
14. Masjedi-Arani M, Salavati-Niasari M. Cd₂SiO₄/Graphene nanocomposite: Ultrasonic assisted synthesis, characterization and electrochemical hydrogen storage application. *Ultrasonics Sonochemistry*. 2018;43:136-45.
15. Sangsefidi FS, Salavati-Niasari M, Mazaheri S, Sabet M.

- Controlled green synthesis and characterization of CeO₂ nanostructures as materials for the determination of ascorbic acid. *Journal of Molecular Liquids*. 2017;241:772-81.
16. Salehabadi A, Salavati-Niasari M, Ghiyasiyan-Arani M. Self-assembly of hydrogen storage materials based multi-walled carbon nanotubes (MWCNTs) and Dy₃Fe₅O₁₂ (DFO) nanoparticles. *Journal of Alloys and Compounds*. 2018;745:789-97.
 17. Mondal S, Rana U, Malik S. Graphene quantum dot-doped polyaniline nanofiber as high performance supercapacitor electrode materials. *Chemical Communications*. 2015;51(62):12365-8.
 18. Zhao Y, Liu M, Deng X, Miao L, Tripathi PK, Ma X, et al. Nitrogen-functionalized microporous carbon nanoparticles for high performance supercapacitor electrode. *Electrochimica Acta*. 2015;153:448-55.
 19. Krishnamoorthy K, Pazhamalai P, Sahoo S, Kim S-J. Titanium carbide sheet based high performance wire type solid state supercapacitors. *Journal of Materials Chemistry A*. 2017;5(12):5726-36.
 20. Acerce M, Voiry D, Chhowalla M. Metallic 1T phase MoS₂ nanosheets as supercapacitor electrode materials. *Nature Nanotechnology*. 2015;10(4):313-8.
 21. Lukatskaya MR, Mashtalir O, Ren CE, Dall'Agnese Y, Rozier P, Taberna PL, et al. Cation Intercalation and High Volumetric Capacitance of Two-Dimensional Titanium Carbide. *Science*. 2013;341(6153):1502-5.
 22. Zhang S, Li Y, Pan N. Graphene based supercapacitor fabricated by vacuum filtration deposition. *Journal of Power Sources*. 2012;206:476-82.
 23. Mai L, Li H, Zhao Y, Xu L, Xu X, Luo Y, et al. Fast Ionic Diffusion-Enabled Nanoflake Electrode by Spontaneous Electrochemical Pre-Intercalation for High-Performance Supercapacitor. *Scientific Reports*. 2013;3(1).
 24. Cui X, Lv R, Sagar RUR, Liu C, Zhang Z. Reduced graphene oxide/carbon nanotube hybrid film as high performance negative electrode for supercapacitor. *Electrochimica Acta*. 2015;169:342-50.
 25. Dreyer DR, Park S, Bielawski CW, Ruoff RS. The chemistry of graphene oxide. *Chem Soc Rev*. 2010;39(1):228-40.
 26. Moon IK, Lee J, Ruoff RS, Lee H. Reduced graphene oxide by chemical graphitization. *Nature Communications*. 2010;1(1).
 27. Cheng Q, Tang J, Ma J, Zhang H, Shinya N, Qin L-C. Graphene and carbon nanotube composite electrodes for supercapacitors with ultra-high energy density. *Physical Chemistry Chemical Physics*. 2011;13(39):17615.
 28. Hummers WS, Offeman RE. Preparation of Graphitic Oxide. *Journal of the American Chemical Society*. 1958;80(6):1339-.
 29. Rasuli R, Mokarian Z, Karimi R, Shabanzadeh H, Abedini Y. Wettability modification of graphene oxide by removal of carboxyl functional groups using non-thermal effects of microwave. *Thin Solid Films*. 2015;589:364-8.
 30. Hosseini F, Rasuli R, Jafarian V. Immobilized WO₃nanoparticles on graphene oxide as a photo-induced antibacterial agent against UV-resistant *Bacillus pumilus*. *Journal of Physics D: Applied Physics*. 2018;51(14):145403.
 31. Ferrari AC, Meyer JC, Scardaci V, Casiraghi C, Lazzeri M, Mauri F, et al. Raman Spectrum of Graphene and Graphene Layers. *Physical Review Letters*. 2006;97(18).
 32. Ferrari AC. Raman spectroscopy of graphene and graphite: Disorder, electron-phonon coupling, doping and nonadiabatic effects. *Solid State Communications*. 2007;143(1-2):47-57.
 33. Malard LM, Pimenta MA, Dresselhaus G, Dresselhaus MS. Raman spectroscopy in graphene. *Physics Reports*. 2009;473(5-6):51-87.
 34. Țucureanu V, Matei A, Avram AM. FTIR Spectroscopy for Carbon Family Study. *Critical Reviews in Analytical Chemistry*. 2016;46(6):502-20.
 35. Abouelhassan S, Salman F, Elmansy M, Sheha E. CHARACTERIZATION OF KHCO₃ SINGLE CRYSTALS. *Surface Review and Letters*. 2004;11(01):83-6.
 36. Yan J, Wei T, Shao B, Ma F, Fan Z, Zhang M, et al. Electrochemical properties of graphene nanosheet/carbon black composites as electrodes for supercapacitors. *Carbon*. 2010;48(6):1731-7.
 37. Wang Y, Chen J, Cao J, Liu Y, Zhou Y, Ouyang J-H, et al. Graphene/carbon black hybrid film for flexible and high rate performance supercapacitor. *Journal of Power Sources*. 2014;271:269-77.
 38. Biswas S, Drzal LT. Multilayered Nano-Architecture of Variable Sized Graphene Nanosheets for Enhanced Supercapacitor Electrode Performance. *ACS Applied Materials & Interfaces*. 2010;2(8):2293-300.
 39. Wang G, Sun X, Lu F, Sun H, Yu M, Jiang W, et al. Flexible Pillared Graphene-Paper Electrodes for High-Performance Electrochemical Supercapacitors. *Small*. 2011;8(3):452-9.